IEEE Access
Multidisciplinary ⋮ Rapid Review ⋮ Open Access Journal

Received 1 March 2024, accepted 6 May 2024, date of publication 8 May 2024, date of current version 16 May 2024.

Digital Object Identifier 10.1109/ACCESS.2024.3399025

RESEARCH ARTICLE

Integrating Machine Learning for Predicting Internal Combustion Engine Performance and Segment-Based CO_2 Emissions Across Urban and Rural Settings

NAGHMEH NIROOMAND[1] AND CHRISTIAN BACH[2]

[1]School of Management and Law, ZHAW Zurich University of Applied Sciences, 8400 Winterthur, Switzerland
[2]Chemical Energy Carriers and Vehicle Systems Laboratory, Swiss Federal Laboratories for Materials Science and Technology (Empa), 8600 Dübendorf, Switzerland

Corresponding author: Naghmeh Niroomand (naghmeh.niroomand@zhaw.ch)

ABSTRACT The assessment of artificial intelligence (AI) application for prediction of internal combustion engine (ICE) performance and its impact on CO_2 emissions is conducted in this paper. Three machine learning techniques (Random Forest, Support Vector Regression, and Semi-supervised Deep Fuzzy C-means) are developed to analyze inputs from an engine simulation software package database. By employing these sophisticated mathematical techniques, we successfully assess the influence of engine power range on CO_2 emissions in this paper. Moreover, the framework facilitates segment-based analysis, which enables segment-specific assessment of CO_2 emission based on metrics such as average traveled distance and average daily trips in urban and rural settings. The Deep Fuzzy C-means model (DFCM) seems promising to predict engine performance, with high predictive accuracy and a coefficient of determination (R^2) approaching unity. The results indicate that integration of inter-class and intra-class distinctions, along with considering the interquartile range of engine power provides invaluable insights for the formulation of strategies aimed at overhauling the passenger vehicle fleet and advancing decarbonization efforts. By implementing the proposed innovative techniques, we aspire to enrich the precision of ICE emission models, leading to more reliable calculations and an enhanced understanding of the environmental implications associated with vehicles.

INDEX TERMS CO_2 emissions, internal combustion engine, passenger car classification, machine learning techniques.

I. INTRODUCTION

In the past decade, there has been a concerning increase in greenhouse gas (GHG) emissions, with an average annual growth rate of 1.3%. The Paris Agreement, adopted over eight years ago [1], set the target of limiting global warming to below 1.5°C. However, it has not yielded positive outcomes. GHG emissions have continued to rise, reaching 53.8 gigatons of carbon dioxide equivalent ($GtCO_2$-eq) in 2022. Surprisingly, the transportation sector alone accounted for 15% (8.7 $GtCO_2$-eq) of these emissions, with a significant 70.1% attributed to land-based modes such as passenger and freight transport. This sector's contribution to global GHG emissions stands at 10% [2]. To tackle the pressing issue of climate change, nations worldwide are formulating tailored strategies for mitigating global warming at various levels of governance. These efforts involve the implementation of context-specific policies aimed at curtailing the impact of climate change on different regions and urban centers. Notable examples include the European Union's pledge to reduce its GHG emissions by 55% by 2030 and achieve carbon neutrality by 2050 [3]. International accords such as the Kyoto Protocol and the Paris Agreement have been established to drive national-scale reductions in GHG

The associate editor coordinating the review of this manuscript and approving it for publication was Jesus Felez.

emissions, promoting the transition to cleaner energy sources and electrified transportation systems. A foundational step in the pursuit of these objectives involves the quantification and comparison of vehicle emissions, providing critical insights into the current state of road transportation in diverse geographic regions [4].

It is noteworthy that despite the implementation of new CO_2 measurement regulations, leading to substantial alterations in the composition of newly immatriculated vehicle fleets and the technical specifications of vehicles over time [5], it is not foreseen to directly impact on-road CO_2 emissions. More specifically, despite significant advancements in technology and strategies such as acquiring new vehicles and decommissioning old or damaged ones, the Swiss passenger car fleet persistently demonstrates elevated CO_2 emissions, exemplified by the cars depicted in Fig. 1, which are indicative of the overall fleet.

Hence, given the slow uptake of alternative fuels in conjunction with a significant rise in the number of passenger vehicles, there is a pressing need to accurately estimate CO_2 emissions across various geographical areas. Researchers have made substantial progress in addressing the discrepancies arising from diverse estimation methodologies. They have employed advanced simulation programs to construct comprehensive emission inventories, thus improving the accuracy and credibility of their findings [6], [7], [8]. These simulation-based strategies effectively overcome the limitations of traditional laboratory testing methods and serve as a crucial bridge between the two primary estimation techniques. In the current context, machine learning models are increasingly relevant in sectors such as energy and automotive technology [9], [10], [11]. Through integrating engine research with machine learning modeling approaches, it is feasible to optimize engine calibration and reduce the dependency on extensive experimentation and Three-dimensional (3D) simulation [12], [13]. In the concept of engines, particularly amidst the progress in technology and changes in characteristics of passenger cars such as engine size and vehicle mass, the promotion of internal combustion engines (ICE) remains active in numerous countries. This persistence is further supported by significant reasons for utilizing machine learning in internal combustion engines, including expediting the development of new engines and lowering costs, particularly in the design of environmentally friendly internal combustion engines [14], [15]. Machine learning offers the capability to adjust input parameters to simulate the combustion characteristics of an engine, thereby forecasting pertinent engine parameters effectively [16], [17]. Intelligent internal combustion engines can analyze a wider array of data inputs, encompassing climate conditions and geographical parameters, to enhance engine efficiency and reduce CO_2 emissions [18]. Dornof et al. [19] examined the influence of European C-segment passenger car models on the comparison of CO_2 emissions under controlled laboratory conditions versus real-world road conditions. The results indicate that CO_2 emissions from diesel-powered vehicles in the same class are quite similar, while gasoline-powered vehicles show significantly lower CO_2 emissions in the same power range. Conventional laboratory experiments are carried out in controlled environments, potentially lacking in capturing the diverse and dynamic variables influencing real-world emissions comprehensively. Conversely, simulation programs facilitate more authentic and dynamic simulations by incorporating a wider array of variables and scenarios [20], [21], [22], [23]. Numerous researchers have employed machine learning methodologies for the anticipation of engine-related parameters. According to Zhang et al [24], the utilization of support vector regression algorithm in numerical simulations has proven to be highly effective in forecasting engine performance and emissions. Karunamurthy et al. [25] conducted a comprehensive review of various machine learning methodologies and algorithms, including artificial neural networks, random forest, semi supervised fuzzy and support vector machine, as utilized by multiple researchers. The discussion in this review delved into an in-depth analysis of performance and emission characteristics of ICEs. The primary objective was to forecast the optimal operational settings to enhance performance and minimize emissions. Yang et al. [26] compared three machine learning models to predictive performance in forecasting indicated mean effective pressure indicator with the input parameters spark timing, speed, and load. For the prediction of engine related parameters, the prediction accuracy and effect of artificial neural networks, random and support vector machine was good. In this research, three machine learning techniques – Random Forest (RF) [27], Support Vector Regression (SVR) [28], and semi-supervised deep fuzzy C-means clustering (DFCM) [29], [30] – will be employed to forecast and enhance the efficiency of engine combustion parameters. Besides mathematically examining the model prediction outcomes, the effectiveness of predictions will also be assessed from the perspective of ICE combustion, enabling the evaluation of engine power range influence on CO_2 emissions via inter-class and intra-class classification. This evaluation considers metrics like average traveled distance and average daily trips in urban and rural settings. The core focus of this study is to construct a robust mathematical model to evaluate average CO_2 emissions for various vehicle class scenarios, providing a more accurate understanding of CO_2 emission levels and shedding light on the influence of vehicle class diversity on the CO_2 footprint of passenger vehicle fleets. Given the limited informative value of CO_2 standard values for real-world emissions [31], this research presents a significant stride towards a renewed approach to assessing CO_2 impacts in vehicle fleet scenarios. This study builds upon previous research that concentrated on developing a machine learning technique for categorizing passenger cars based on technical and dimensional attributes [32], [33], [34].

The rest of the paper is structure as follows. Section II briefly introduces the Swiss transport, Section III provides concise details on the used datasets and the methods,

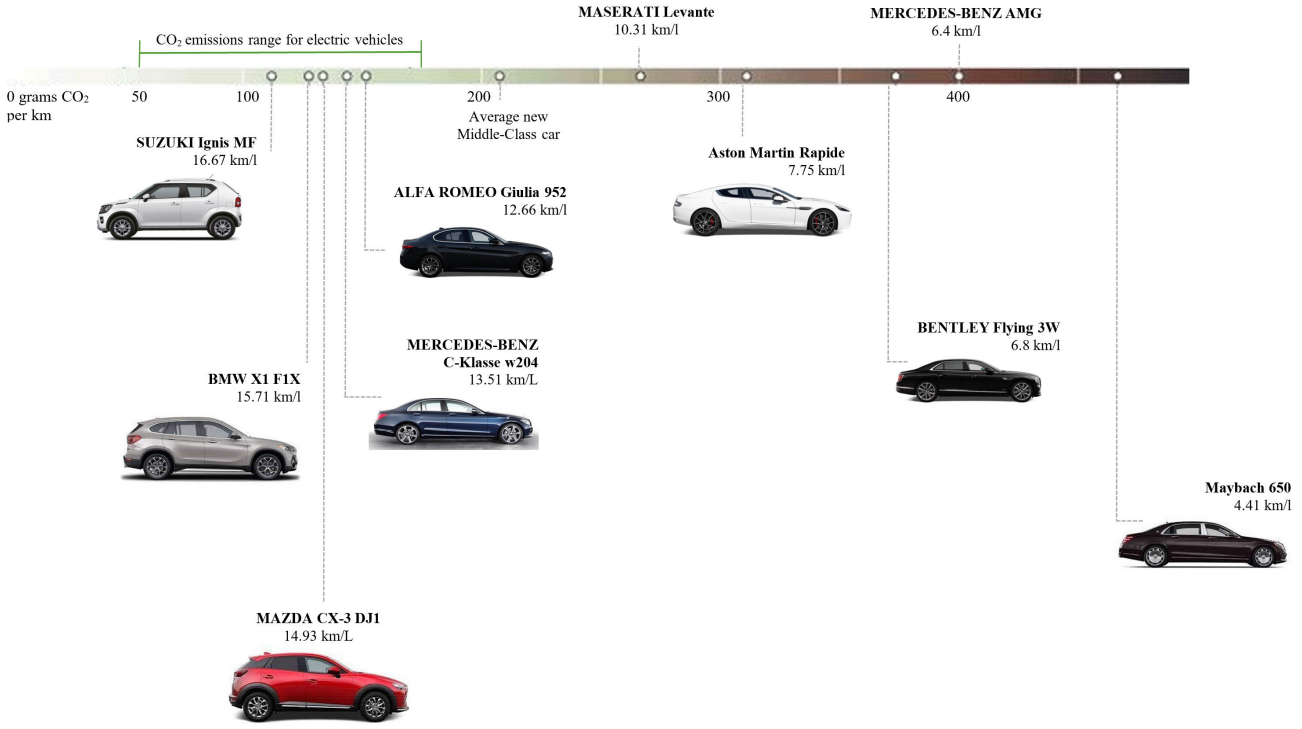

FIGURE 1. CO_2 emission for selected Swiss passenger cars. Data source: ASTRA (Technical data), BFE (CO_2 enforcement data).

Section IV describes the algorithms, the performed experiments, and the discussion of the results and last, section V provides the majors findings of our work and recommendations for further research.

II. SWISS TRANSPORT: A REGIONAL PERSPECTIVE

Based on data from the International Energy Agency [35], Switzerland's share of global human-caused CO_2 emissions resulting from fossil fuels is below 0.2%. Despite this, the transportation sector notably influences Switzerland's overall carbon footprint, with about 30.6% of the country's CO_2 emissions in 2021 stemming from transportation activities. Within transportation modes, road transport is the predominant source, contributing to 97.3% of these emissions. Passenger vehicles constitute a significant portion of Switzerland's road transport emissions, accounting for around 71.2% of the total emissions [36]. Notably, the regulated CO_2 emissions from passenger cars in Switzerland display a variable pattern. Nevertheless, Switzerland has set a long-term target of achieving net-zero greenhouse gas emissions by 2050 by employing negative emission technologies, as depicted in Fig. 2. In 2023, Switzerland recorded the registration of over 6.6 million motor vehicles. Among these, more than 4.7 million were passenger cars. Despite a high public transport acceptance rate of 59% in the population, car travel remains dominant, constituting around two-thirds of the total passenger kilometers traveled [37]. Switzerland's mobility can be segmented into three primary regions - urban, suburban, and rural areas, each facing distinct sustainability challenges stemming from urbanization. According to the Federal Office for statistics (BFS) typology "Area with urban character, 2012", urban areas are categorized into three main estimates: urban core areas, areas of influence of urban cores, and areas outside the influence of urban cores [37]. The classification helps distinguish the different characteristics and dependencies of urban, suburban, and rural areas. Throughout 2023, these vehicles collectively covered a distance of 55 billion kilometers annually, averaging 20.8 kilometers per day. According to the Federal Office for Spatial Development, this translates to a rate of 100,000 kilometers per minute. For journeys exceeding one kilometer, on average, 92% of individuals used passenger cars. The urban-rural disparities are highlighted in Fig. 3 when examining cantons. Urban cantons such as Geneva and Basel-Stadt exhibit the shortest daily travel distances, with values of 18.3 km and 19.7 km respectively, while Alpine cantons like Uri and Valais show considerably greater distances. Fribourg stands out with an average daily distance of 37.2 km, contrasting with the relatively shorter distance of 24.1 km in Ticino [38]. Furthermore, vehicles powered by diesel and gasoline engines typically covered greater annual distances compared to those equipped solely with electric motors or hybrid systems, as depicted in Fig. 4. This resulted in an average type-approval CO_2 emission of approximately 120.9 g CO_2/km for newly registered vehicles in 2022. The transition to

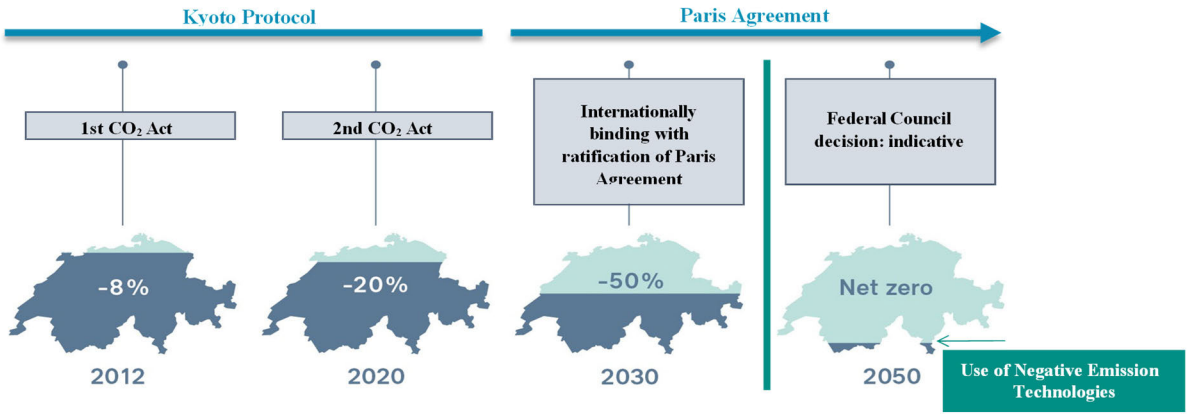

FIGURE 2. Overview of CO_2 emission targets in Switzerland, Source: BAFU (long-term climate strategy).

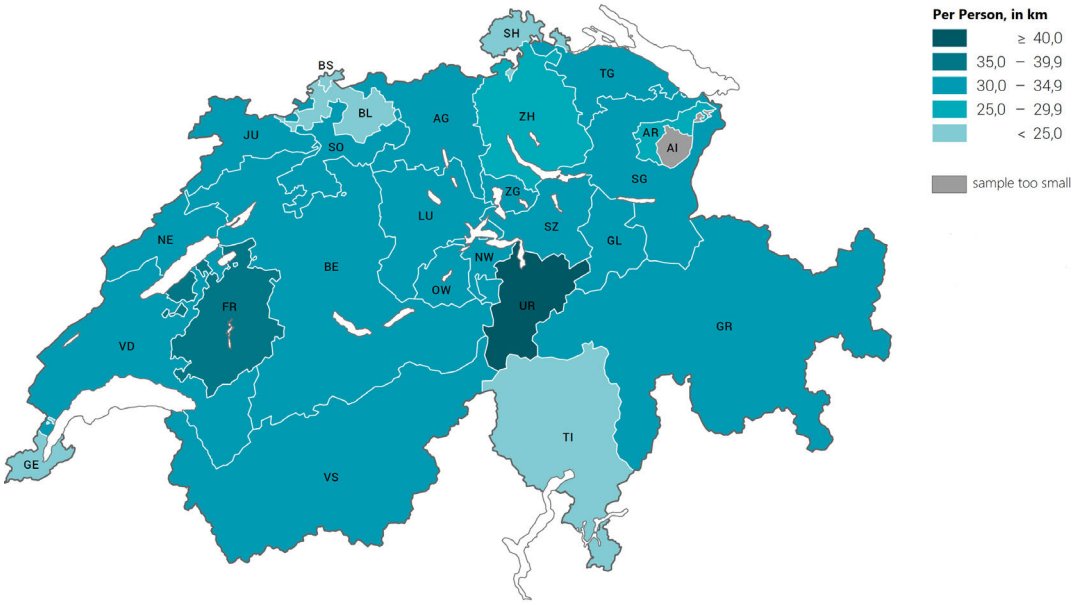

FIGURE 3. The daily travel distances in urban and rural areas, Data Source: BFS (statistics/mobility-traffic).

the World Harmonized Light-Duty Vehicles Test Procedure (WLTP) unveiled an average 20% increase in emissions compared to the New European Driving Cycle (NEDC) standards [39]. Additionally, the estimated emissions indicate that newly registered vehicles in the southeastern region of the country generally demonstrate lower fuel efficiency and higher CO_2 emissions compared to those in the northwest [37].

III. MATERIALS AND METHODS

A. DATA PREPARATION

In this study, we undertook a comprehensive analysis utilizing the extensive dataset sourced from the Swiss Motor Vehicle Information System (MOFIS), which encompasses detailed records of over 4.7 million passenger vehicles [40]. The dataset contains a plethora of attributes including type approval numbers, physical specifications, weight properties, ownership details, technical specifications, and registration timelines. Furthermore, we augmented this dataset with information from the Technical Type Approval Information repository provided by the Federal Roads Office (ASTRA) [41] and the Vehicles Expert Partner [42]. It is important to note that we used CO_2 emissions based on the average type approval values provided in the ASTRA database (measured CO_2 according to WLTP) [33]. The data cleaning and preliminary analysis are conducted using Python [34]. Our primary objective revolved around partitioning the dataset into a meticulously crafted training set and a robust testing set, with the former comprising 312,377 newly registered passenger cars in the year 2019. Out of this total, 192,430 were diesel-

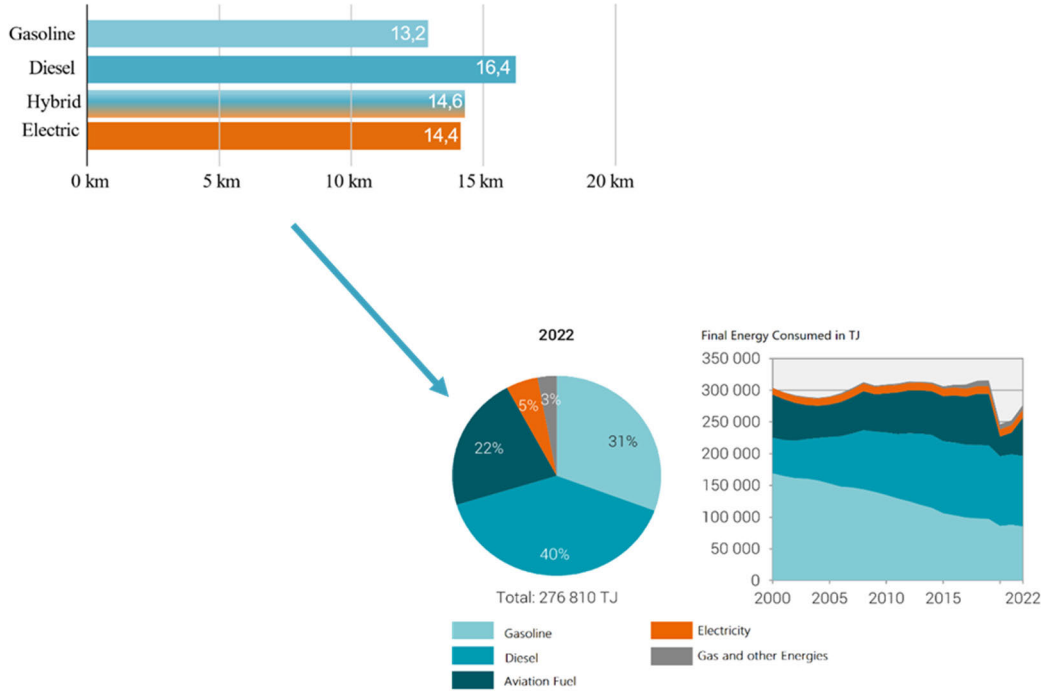

FIGURE 4. The daily travel distances by fuel type, Data Source: BFS (statistics/mobility-traffic).

powered passenger cars, and 76,618 were gasoline-powered passenger cars, representing the collective share of diesel and gasoline vehicles in the dataset. Following a stringent filtering process to remove the vehicles that do not meet the standard definitions of passenger cars, we proceeded to categorize the remaining automobiles into distinct types based on their make, model, and manufacturer code, resulting in the identification of 378 unique passenger car types. These types were systematically grouped into specific classes, presenting the diversity within the passenger car mathematical segment, including the micro class, small class, middle class, upper middle class, and large and luxury class. Given the inherent constraints of the unsupervised Fuzzy C-means (FCM) clustering algorithm [30], our methodology necessitated the exclusive utilization of labeled data exhibiting precise labels and a high membership degree exceeding 0.95. This meticulously constructed central dataset functioned as the pivotal element for deriving precise categorizations and establishing the foundational framework for ensuing training procedures. In addition, a deliberate random sampling approach was utilized, designating 10% of data from each category as labeled training samples. Subsequently, we elaborate on the process of estimating the actual power output and its effect on CO_2 emissions assessment based on the average traveled distance and determining the average daily trips in urban and rural area.

B. STATE-OF-THE-ART METHODS

Semi-supervised clustering aims to boost cluster accuracy by identifying superior clusters compared to those obtained via unsupervised learning algorithms [43], [44], [45]. Traditionally, semi-supervised clustering methods deliver suboptimal outcomes in the original feature space. To enhance the efficacy of semi-supervised clustering, incorporating deep feature learning is a logical step [29], [46], [47]. The framework of the proposed clustering approach is illustrated in Fig. 5.

In contrast to prevalent methodologies in semi-supervised clustering that hinge on feature extraction techniques, our approach integrates three types of information (diffusion labels, core data extraction, and feature vector extraction) to enhance prediction accuracy and address issues like imbalanced class distribution and class overlap. Our framework comprises three key layers, with the initial layers discussed in a previous study [33]. In the first layer, we segregate labeled data into distinct training and testing sets for building and evaluating classifiers, respectively. The second layer involves using the training set and unlabeled data as inputs for the feature learning process. The outcome of this step generates cluster centroids, which act as a foundation for projecting data from both training and testing sets into a newly acquired space. This projection further facilitates the extraction of feature vectors during the subsequent feature extraction phase. In the second layer of the study, models are constructed RF, SVR, and DFCM algorithms based on the feature vectors extracted from the training dataset. These models are subsequently leveraged to forecast labels for the corresponding feature vectors within the testing dataset. In algorithm 1, RF employs parallel learning and utilizes bagging during data training to reduce both variance and

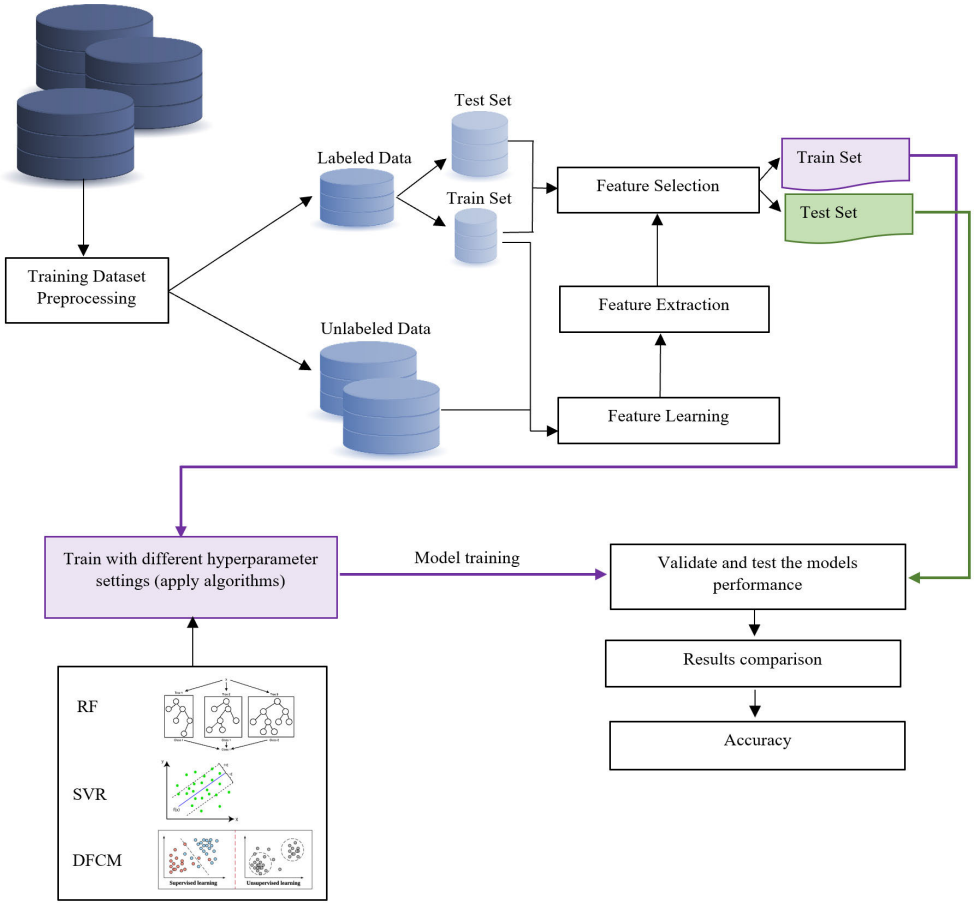

FIGURE 5. Overall Structure of the proposed deep learning approach.

bias in the model. This technique generates multiple decision tree ensembles from the original data while ensuring that these trees remain independent of each other throughout the parallel learning process.

Algorithm 1 Random Forest

Input: Training set (S), number of decision trees in the forest (B), subsample size (μ), maximum iteration number (T)
Output: Set K = $\emptyset$
1. Initialize the iteration number t ϵ {1, . . . , T} do
2. For each decision tree index b ϵ {1, . . . , B} do the following steps:
   a) Sample μ instances from S with replacement, creating a subsample set S_t
   b) construct a decision tree K_t using decision tree b on the subsample set St
   c) Add the trained decision tree classifier K_t to set K
3. Return the set K

Algorithm 2 Support Vector Regression

Input: Data X whose number of elements N, training set (S), Kernel function (K), regularization parameter (C), epsilon insensitive loss parameter (ε), max iteration number (T)
Output: Set Q = $\emptyset$
1. for t ϵ {1, . . . , T} do
2. Initialize α, b, and Q
3. for each training instance x_i:
4. Calculate the prediction error $\varepsilon_i = y_i$ - ($\Sigma_j \alpha_j K(x_j, x_i)$ + b)
5. Update α_j according to the rule:

$$\alpha_i \leftarrow \alpha_j + \eta(\varepsilon_i - \varepsilon_b)K(x_b, x_b)$$

6. Update b: b $\leftarrow$ b + ε_i
7. if convergence criterion is satisfied, then stop
9. Update the set Q
10. Return the set Q

In algorithm 2, SVR is a favorable choice in machine learning for addressing intricate regression tasks with non-linearity. It predicts continuous target variables by identifying the hyperplane that optimally maximizes the margin between data points and the hyperplane. Unlike the sequential creation of decision stumps, SVR centers on grasping the connections between input variables and the continuous target variable by utilizing support vectors during the training phase.

FCM is a widely used soft clustering algorithm known for its overlapping clusters [29]. It assigns partial membership values to data points, indicating their likelihood of belonging to each cluster on a scale from 0 to 1. However, due to the non-convexity of its objective function, FCM may converge to local optima during optimization. To tackle this challenge, In algorithm 3, we propose a DFCM that incorporates deep feature learning to enhance its effectiveness and eliminate redundant information [44], [48]. To enhance prediction accuracy and performance, we employ the random oversampling (ROS) technique for feature selection. ROS aims to strike a balance between the feature subsets of labeled classes and unlabeled data elements, thereby improving the prediction process [49], [50].

Algorithm 3 Semi Supervised Deep Fuzzy C-Means

Input: N data elements $X = \{X_1, X_2, \ldots, X_N\}$ with minimum features in any subset (s), set of the centroid (V_{iL}^{s}, V_{UNL}^{s}) of selected features

Output: Predicted labeled data ($Q = \{q_{L+1}, q_{L+2}, \ldots, q_{L+N}\}$)

Set $Q = \emptyset$

1. For each centroid index $i \in \{1, \ldots, c\}$ do
2. For each data element index $j \in \{1, \ldots, N\}$, do the following steps:
   a) Employ V_{iL}^{s} to calculate $max\ Sim_i$
   b) If maximum average of $max\ Sim_i \in i^{th}$ labeled class, then
   c) Append X_j to i^{th} labeled class
   d) Update the set Q if a labeled class is achieved
   e) For all $V_{iL}^{s} \in V_L^{s}$ do
3. Return the set Q

Confusion Matrix

Actual Value	Predicted Value (class i): Positive	Predicted Value (class i): Negative	
Positive	*True Positive Prediction (TP)*	*False negative prediction (FN)*	Recall (R_i) $\frac{TP_i}{TP_i+FN_i}$
Negative	*False Positive Prediction (FP)*	*True negative prediction (TN)*	Specificity $\frac{TN_i}{TN_i+FP_i}$
	Precision (P_i) $\frac{TP_i}{TP_i+FP_i}$	Negative Predictive $\frac{TN_i}{TN_i+FN_i}$	F-Measure $\frac{2P_iR_i}{P_i+R_i}$

Rand Index	$\frac{TP+TN}{TP+FN+TN+FP}$	$(0 \le RI \le 1)$
Adjusted Rand Index	$\frac{RI-E[RI]}{\max(RI)-E[RI]}$	$(-1 \le ARI \le 1)$

In the final layer of the process, we assess the performance metrics of the distinct models (RF, SVR, DFCM) through the utilization of the confusion matrix. Additionally, we employ a fusion model to gauge their efficacy in data classification and prediction. The fusion model is a sophisticated deep learning approach where diverse prediction algorithms, each assigned specific weights, are trained, and amalgamated to enhance overall performance. This method proves to be a robust meta-classifier as it integrates various prediction models using a majority voting classifier, thereby mitigating the limitations of individual classifiers, and achieving heightened prediction accuracy [22], [51]. Subsequently, the findings from the experiments are applied to a dataset for deeper scrutiny and validation.

IV. EXPERIMENTS

A. EXPERIMENTAL SETUP AND RESULTS

This section delves into comparing the robustness and performance of three machine learning algorithms (RF, SVR, and DFCM) for predicting ICE power output for each vehicle segment. The approach employed in this study to evaluate the capability of machine learning algorithms in predicting engine performance involves conducting the engine simulation with diverse engine inputs including spark ignition, spark timings, engine capacity, engine speed, load, and torque, and recording the resulting performance outcomes. The engine input parameters sourced from the simulation package database serve as inputs for the algorithms. The majority of the pre-existing data within the database has been validated through dyno tests, leading to the anticipation that the simulation outcomes accurately reflect actual engine performance. To assess their robustness, the models were trained and validated multiple times, and the resulting data was analyzed for its impact on CO_2 emissions. Initially, a statistical analysis indicated a strong correlation between CO_2 emissions, vehicle segments, sub-segments, and key influencing factors. During the feature learning process, both labeled and unlabeled data were utilized along with core dataset labels, ensuring common features across datasets. Principal component analysis was employed to tackle multicollinearity before feature extraction to reduce dimensionality. Cluster centroids defined features which were then transformed into feature vectors. The random oversampling technique was used to balance minority group features with the majority group, selecting optimal features based on Euclidean distance to minimize redundancy. Pseudo labels from labeled data were assigned to unlabeled data for training, and the resultant pseudo-labeled data was used to pre-train the algorithms by extracting discriminative features. Model fusion was undertaken using labeled data with true labels. The results revealed that the DFCM algorithm achieved the highest accuracy (Table 1). The features extracted from model fusion were then used to reevaluate individual algorithms and choose the best prediction model. The experimental findings demonstrate the superior capability of the DFCM algorithm in extracting valuable insights from the vehicle dataset, resulting in enhanced recognition accuracy when compared to alternative prediction algorithms. The underlying assumption of feature extraction is that it leads to improved prediction

TABLE 1. Comparison of performance of the prediction algorithms with labeled rate of 10% from training dataset.

Machine Learning	Model	Feature Learning Techniques		Feature Extraction Techniques	
		Accuracy Rate	Precision Rate	Training Accuracy	Test Accuracy
Algorithm 1	SVR	0.913	0.904	0.956	0.973
Algorithm 2	RF	0.881	0.876	0.864	0.851
Algorithm 3	DFCM	0.968	0.952	0.973	0.982

results in comparison to the initial classifier's predictions with the original features.

Fig. 6a to 6c present the outcomes of comparing actual values with predicted outputs obtained from the RF, SVR, and DFCM algorithms using 378 distinct sets of training data tailored for passenger cars. The X and Y axes represent the predicted and actual power output values derived from the measured technical features, including spark ignition, spark timings, engine capacity, engine speed, load, and torque, across various vehicle categories. The high value of R2 signifies an accurate prediction. Examination of the error lines, set at ±5% and ±10%, reveal that the data points produced by the SVR algorithm closely adhere to the diagonal line. DFCM trails closely behind, while the RF algorithm displays the most significant deviation. Both DFCM and SVR classifier exhibit robust R^2 values exceeding 97%. Additionally, both DFCM and SVR exhibit higher precision rates compared to the RF classifier, suggesting improved prediction accuracy after training. Overall, all three prediction classifiers display high R^2 values, indicating their understanding of the relationship between engine performance and input parameters, with DFCM and SVR outperforming the RF classifier.

Transitioning to Fig. 6d to 6f, these illustrations present a comparison between anticipated power output and actual values for the validation dataset utilizing the three algorithms. The resemblances in statistical metrics between the validation and training datasets for each algorithm indicate minimal fluctuations in R^2 values, signaling the absence of overfitting and a reliable capacity to predict unseen data. The validation dataset displays R^2 values of 0.982, 0.978, and 0.968 for DFCM, RF, and SVR classifiers correspondingly. R^2 values surpassing 0.98 for both DFCM and SVR denote high accuracy in their predictive abilities. Notably, the prediction errors for the SVR algorithm predominantly fall within the 5% margin in the validation dataset, whereas for the DFCM algorithm, errors hover within 10%, with only a scarce number of points exceeding the 10% errors. Conversely, the RF classifier present more conspicuous prediction errors surpassing the 10%. The experimental results affirm that the DFCM classifier exhibits the closest alignment with actual values in its prognostications, with SVR following, while the RF classifier displays relatively higher errors compared to the DFCM and SVR classifiers.

Consequently, the inter-class classification outcomes derived from the DFCM algorithm are applied to a dataset consisting of passenger cars [30]. This analysis reveals the presence of seven distinct classes, each characterized by their predicted power output and corresponding engine capacity. These class distinctions, documented in detail in Table 2, provide valuable insights into the segmentation and characterization of passenger cars based on their attributes and performance metrics. Moreover, the visualization depicted in Fig. 7 illustrates the spatial distribution of predicted power output within diverse urban and rural settings. Analysis of the data discerns that rural and urban cantons exhibit a prevalence of passenger cars with power output levels situated within the lower quartile range. Conversely, urban and semi-urban regions present a notably higher concentration of vehicles in the upper quartile power output segment among small vehicle classifications, accounting for over 44%, with the upper-middle class sector contributing significantly at 30%. Furthermore, middle quartile power output predominates among the upper-middle class in semi-rural and rural regions, exceeding 40%. Furthermore, the examination of drivetrain technologies in vehicles classified into five distinct classes (micro, small, midsize, upper midsize, large and luxury) reveals that over two-thirds of SUVs utilize four-wheel drive (4WD), while the majority of not-SUV models utilize front-wheel drive (FWD) or rear-wheel drive (RWD). Among the unique training data across the five main inter-class categories, only 156 samples fulfill the 4WD criteria. Subsequently, based on dataset assessment, SUVs encompass merely 96 samples, with not-SUVs accounting for 282 samples. The DFCM achieves 91% accuracy in intra-class vehicle classification with just 10% labeled data. An observable trend surfaces, indicating a higher prevalence of SUVs in the central and southern regions.

B. DISCUSSIONS

The experiment results have demonstrated that there is a significant variation in the CO_2 emissions between inter and intra classes. The cumulative CO_2 emission levels from Swiss passenger cars are notably influenced by alterations in the fleet's composition over time, both between vehicle classes (e.g., upper-middle class to large and luxury classes) and within each class (e.g., not-SUV to SUV). Fig. 8 presents the average CO_2 emissions for each vehicle category based on our prediction methods. The outcomes for each vehicle class are depicted using interquartile range distributions of engine power output. A comparative analysis of different vehicle segments highlights a substantial variance in CO_2 emissions

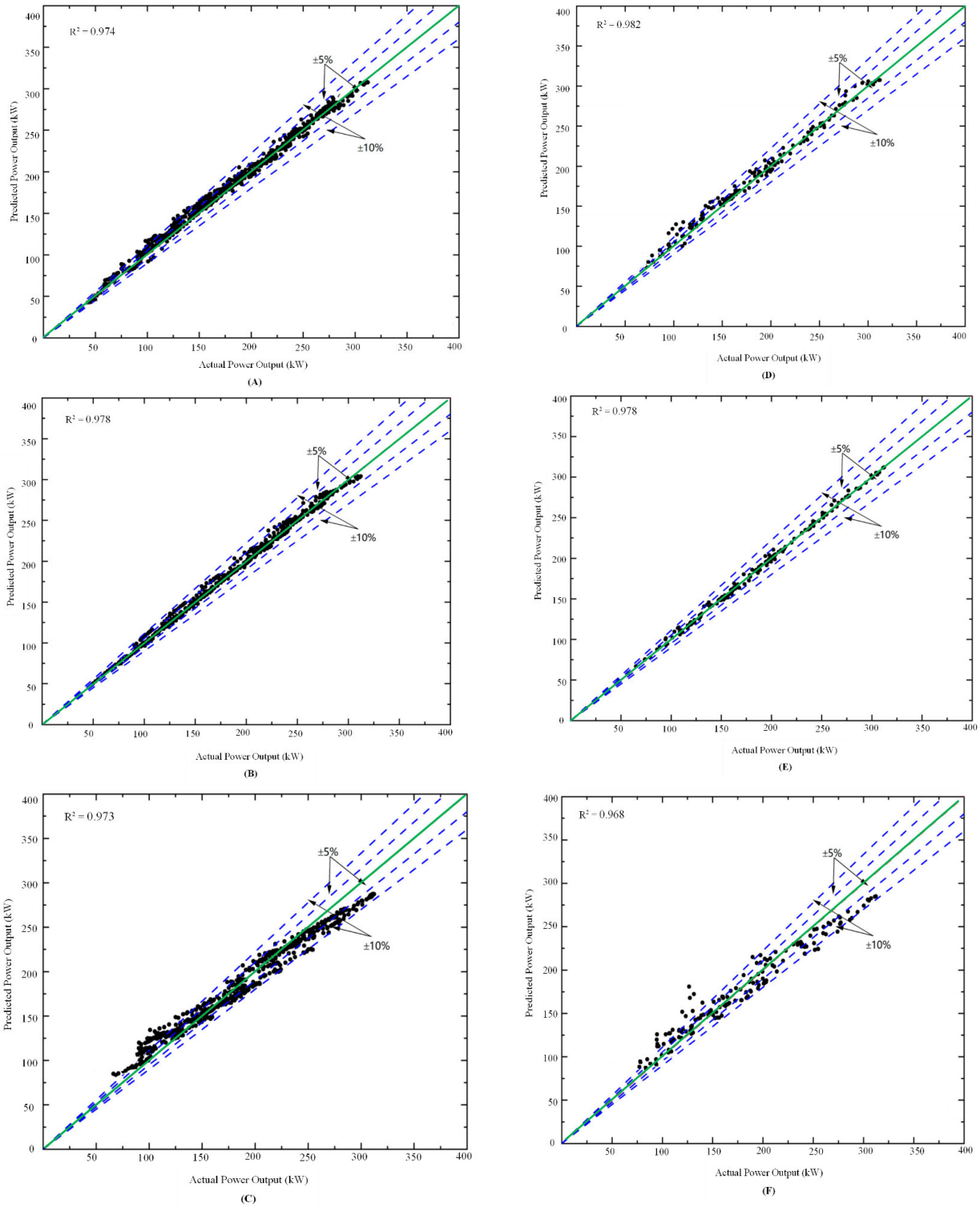

FIGURE 6. A comparative analysis of the predicted power output against actual values using the proposed algorithms. It includes visual representations of the performance for the training dataset by (A) DFCM, (B) SVR, and (C) RF. Additionally, a validation process was carried out using 10% of the training dataset samples for model training, presenting the predicted performance for the validation dataset by (D) DFCM, (E) SVR, and (F) RF.

within and between classes. There is a tendency for CO_2 emissions to increase with the size of the vehicle, ranging from approximately 100 g CO_2/km for micro-class vehicles to around 200 g CO_2/km for large and luxury-class vehicles. Specifically, SUVs exhibit higher CO_2 emissions compared to not-SUVs, with the most significant variance noted in

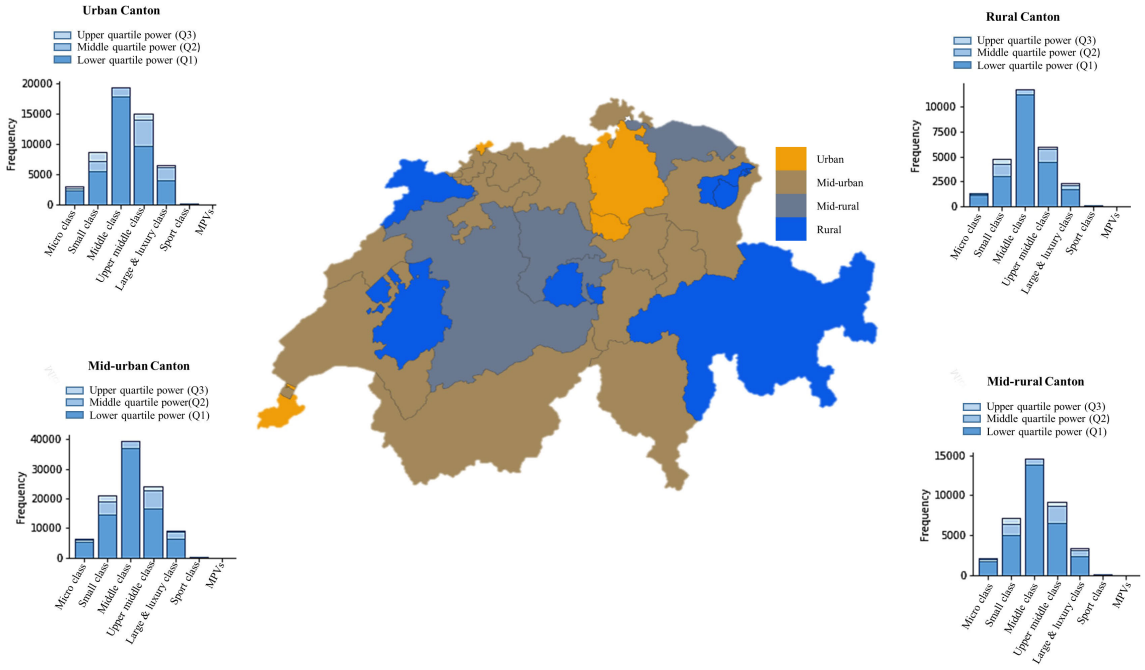

FIGURE 7. Spatial distribution of the power range in kW for each area and car segmentation in 2019.

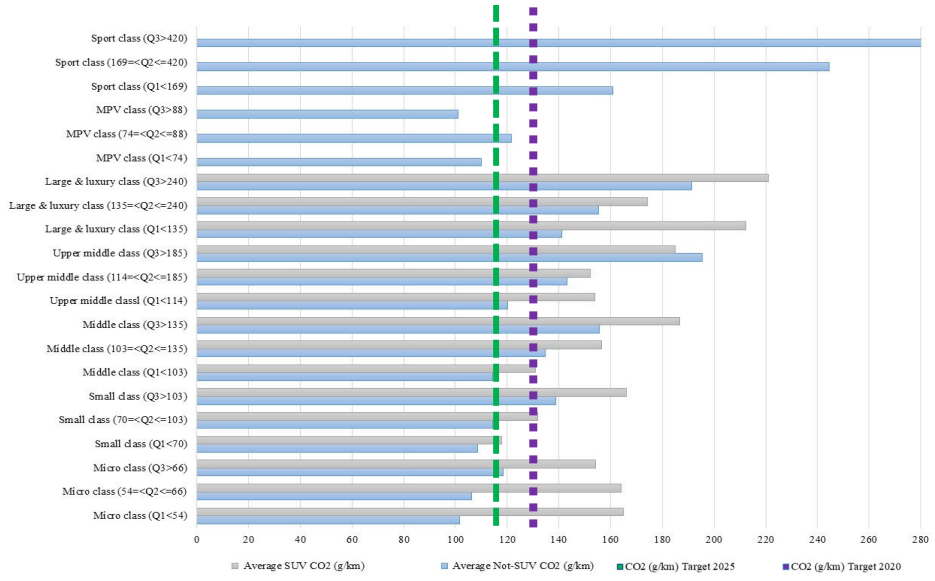

FIGURE 8. Average CO_2 emissions intensity based on the interquartile power range.

micro-class SUVs as indicated in Fig. 9. Additionally, our related observations revealed that the average mileage of SUVs tends to increase as vehicles age. This notable finding highlights that the SUV fleet in Switzerland covered an extensive distance of 12.6 billion kilometers in 2018, resulting in the unnecessary production of CO_2 emissions with each kilometer traveled [34].

The findings indicate that transitioning from a mid-class not-SUV to a micro-class SUV could lead to an increase in CO_2 emissions. Therefore, while transitioning the fleet towards smaller vehicles may reduce CO_2 emissions, a more effective reduction in emissions intensity could be achieved by adjusting the proportion of vehicles within each class based on the interquartile range of engine power, for instance shifting from SUVs to not-SUVs or selecting lower-power vehicles within the same vehicle class, as indicated in Fig. 8.

Furthermore, as discussed in the preceding section, the analysis of CO_2 emissions is greatly influenced by driving distances and vehicle classes. Hence, the utilization of driving distances derived from statistically averaged data

TABLE 2. Power output quartile analysis of the clustering results derived from the DFCM classifier.

Vehicle classes	Average power output (kW)	Engine capacity
Class representatives: SMART Fortwo 451, TOYOTA Aygo AB1, FIAT 500 312, SUZUKI Jimny FJ		
Micro class	(Q1<54), (54=<Q2<=66), (Q3>66)	(Q1<898), (898=<Q2<=1242), (Q3>1242)
Class representatives: VW Polo AW, AUDI S1 8X, ALFA ROMEO MiTo 955, SUZUKI Vitara LY		
Small class	*(Q1<70), (70=<Q2<=103), (Q3>103)*	(Q1<999), (99=<Q2<=1242), (Q3>1497)
Class representatives: DACIA Duster SR, TOYOTA C-HR AX1, ALFA ROMEO Giulietta 940, VW Tiguan 5N		
Middle class	(Q1<103), (103=<Q2<=135), (Q3>135)	(Q1<1461), (1461=<Q2<=1798), (Q3>1995)
Class representatives: SKODA Octavia 5E, ALFA ROMEO Giulia 952, AUDI A4 B8, HYUNDAI Santa TM		
Upper middle class	(Q1<114), (114=<Q2<=185), (Q3>185)	(Q1<1968), (1968=<Q2<=2488), (Q3>2488)
Class representatives: AUDI A6 4G, BMW 5er G5L, MERCEDES-BENZ AMG 212, AUDI Q7 4L		
Large & luxury class	(Q1<135), (135=<Q2<=240), (Q3>240)	(Q1<1984), (1984=<Q2<=2993), (Q3>2993)
Class representatives: FORD Tourneo JU2, VW Caddy 2K		
MPV class	(Q1<74), (74=<Q2<=88), (Q3>88)	(Q1<998), (998=<Q2<=1499), (Q3>1499)
Class representatives: ASTON MARTIN Rapide, BENTLEY Continental 3S		
Sport class	(Q1<169), (169=<Q2<=420), (Q3>420)	(Q1<1998), (1998=<Q2<=3993), (Q3>3993)

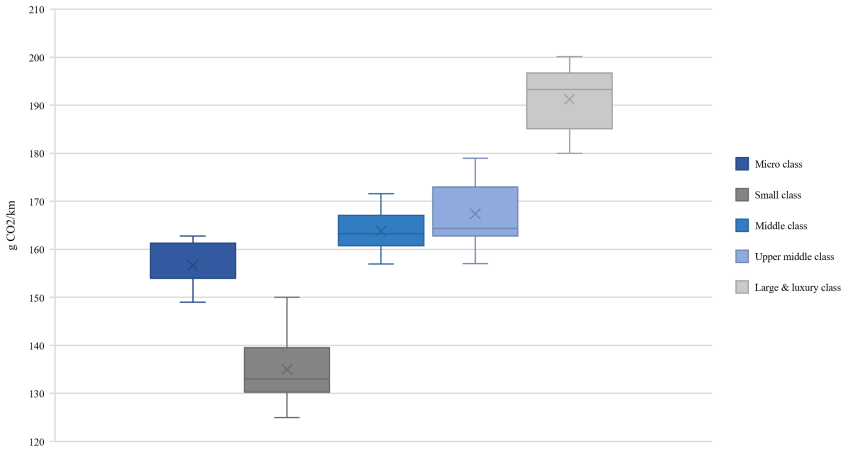

FIGURE 9. The box plot depicts the average CO_2 emissions fluctuation among different segments of SUV passenger cars, representing median and 25/75% quartiles, and the mean (×) of the CO_2 emissions.

sources is imperative to accurately evaluate the comparative CO_2 emission levels across different vehicle classes within the respective region. In the context of 2021, passenger cars were driven almost three-quarters more than other transportation alternatives. Diesel-powered passenger cars exhibiting slightly longer annual distances traveled (12,782

km) compared to gasoline-powered counterparts (9,010 km), partly attributed to the relative age differences of the vehicles within each fuel category [33]. Moreover, highest percentage of registered SUVs is observed in four urban and mid-urban cantons (Zug, Schwyz, Genèva and Valais) in compared to the lowest percentage of registered SUVs which is observed in rural and mid-rural cantons (Thurgau, Freiburg, Neuchâtel, and Jura). Our analysis of the environmental impact of SUV transportation in cantons Genèva and Freiburg, as presented in Fig. 10, revealed some insightful findings. Despite there being no technical differences between the vehicles analyzed in each setting, it is possible to highlight that an average kilometer trip made by registered SUVs with ICE in Genèva brings approximately 166 g CO_2/km with 5.8 km average travel distance per person per day. Conversely, for SUVs operating in canton Freiburg, where the average travel distance per person per day is 4.7% lower than in canton Genèva, the emissions are slightly reduced to 161 g of CO_2 per kilometer. Despite this, canton Freiburg boasts the highest average daily travel distance per person among the 26 cantons considered, leading to significant variations in CO_2 emissions both within and between vehicle classes. Consequently, the integration of inter-class and intra-class distinctions, coupled with the consideration of the interquartile range of engine power provides invaluable insights for the formulation of strategies aimed at overhauling the passenger vehicle fleet and advancing decarbonization efforts. It worth noting that the lower distances observed in the border regions may be influenced by residents who tend to travel slightly longer distances abroad in their daily routines, and this analysis specifically considers distances within the country.

By leveraging an established estimation-based model from a different country [52], a comparative analysis was carried out using actual data from Switzerland. It's important to note that direct comparisons between countries with different driving fleets, behaviors, road infrastructures can be complex. However, such comparisons offer valuable insights into key differences. The findings reveal that vehicles in Switzerland significantly exceed the targeted CO_2 emissions levels. This study suggests that as the transition to alternative fuels progresses slowly, there is an opportunity to mitigate CO_2 emissions by optimizing power range and vehicle classes. By strategically matching power range with vehicle classifications, a more immediate reduction in CO_2 emissions can be achieved, paving the way for a smoother transition towards sustainable fuel sources. For instance, two variants of the gasoline-powered Golf TSI, both sharing the same base engine and speed but with power outputs of 96 kW and 110 kW, respectively exhibited CO_2 emissions of approximately 111 g/km and 119 g/km. It is worth noting that analogous middle-class vehicle models from other manufacturers with the similar power output of 96 kW and maximum speed of 210 km/h displayed considerably higher CO_2 emissions, such as the BMW 118i with 140 g CO_2/km and the Peugeot 308 with 124 g CO_2/km [19].

V. CONCLUSION

Numerous research has employed machine learning algorithms to predict and optimize engine parameters in addressing global climate change. These studies have demonstrated the effectiveness of integrating machine learning techniques in engine performance domain tasks. Nevertheless, a com-

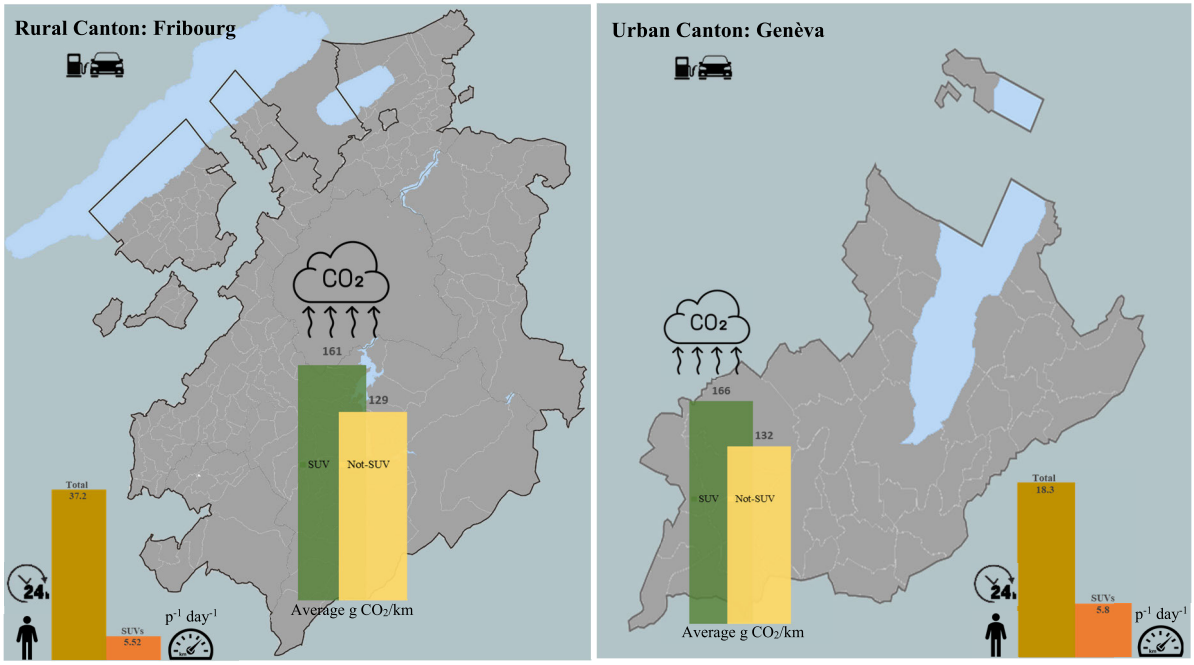

FIGURE 10. A comparison of CO_2 emissions in selected urban and rural areas.

mon trend among researchers has been the singular focus on assessing the predictive capabilities of individual models, overlooking the value of comparing outcomes derived from a range of models. In this study, an exploration encompassing three distinct machine learning algorithms – SVR, RF, and DFCM – has illuminated the potential for AI to proficiently predict engine performance across an array of geometries and operational scenarios while evaluating their impact on CO_2 emissions utilizing engine technical inputs as principal parameters. The comparison revealed that both DFCM and SVR exhibited similar levels of prediction accuracy and effectiveness, surpassing the performance of RF within the context of this investigation. Among the classifiers evaluated, the DFCM algorithm emerged as the most precise, achieving a classification accuracy of 98% in validation assessments. This study primarily delved into assessing the influence of engine power range on CO_2 emissions through inter-class and intra-class classification based on metrics such as average traveled distance and average daily trips in urban and rural settings. The findings underscored notable disparities in average CO_2 emissions across various vehicle classes. While transitioning the vehicle fleet towards smaller vehicle classes may lead to reduced CO_2 emissions, a more substantial decrease in emission intensity could be attained by reconfiguring the distribution of vehicles within each class towards the lower interquartile engine power range or by interchanging vehicle classes based on power output thresholds, such as converting SUVs to not-SUVs. Hence, the proposed methodologies offer crucial insights for formulating strategies to shift the passenger vehicle fleet towards decarbonization while enabling precise automated classification of large vehicle databases, facilitating the analysis of fleet modifications. A promising direction for future research involves integrating CO_2 estimates derived from real-world measurements to provide a more precise evaluation of fleet CO_2 emissions from a life-cycle emissions perspective.

ACKNOWLEDGMENT

The authors would like to thank the Federal Roads Office (FEDRO) for providing the Swiss Vehicle Information System (MOFIS) data and the vehicle technical dataset and the Vehicle Expert Partners for providing the expert segmentation data.

REFERENCES

[1] *The Paris Agreement | UNFCCC*. Accessed: Jan. 2024. [Online]. Available: https://unfccc.int/process-and-meetings/the-paris-agreement/the-paris-agreement

[2] (2023). *Intergovernmental Panel on Climate Change (IPCC) Synthesis Report of the IPCC Sixth Assessment Report (AR6)*. Accessed: Jan. 2024. [Online]. Available: https://www.ipcc.ch/report/sixth-assessment-report-cycle/

[3] E. Dorr, C. François, A. Poulhès, and A. Wurtz, "A life cycle assessment method to support cities in their climate change mitigation strategies," *Sustain. Cities Soc.*, vol. 85, Oct. 2022, Art. no. 104052, doi: 10.1016/j.scs.2022.104052.

[4] Y. Kazancoglu, M. Ozbiltekin-Pala, and Y. D. Ozkan-Ozen, "Prediction and evaluation of greenhouse gas emissions for sustainable road transport within Europe," *Sustain. Cities Soc.*, vol. 70, Jul. 2021, Art. no. 102924, doi: 10.1016/j.scs.2021.102924.

[5] *European Commission. Reducing CO_2 Emissions From Passenger Cars*. Accessed: Jan. 2024. [Online]. Available: https://ec.europa.eu/clima /policies/transport/vehicles/cars_en

[6] J. Pavlovic, K. Anagnostopoulos, M. Clairotte, V. Arcidiacono, G. Fontaras, I. P. Rujas, V. V. Morales, and B. Ciuffo, "Dealing with the gap between type-approval and in-use light duty vehicles fuel consumption and CO_2 emissions: Present situation and future perspective," *Transp. Res. Rec., J. Transp. Res. Board*, vol. 2672, no. 2, pp. 23–32, Dec. 2018.

[7] H. Dai, P. Mischke, X. Xie, Y. Xie, and T. Masui, "Closing the gap? Top-down versus bottom-up projections of China's regional energy use and CO_2 emissions," *Appl. Energy*, vol. 162, pp. 1355–1373, Jan. 2016.

[8] P. Thunis, B. Degraeuwe, K. Cuvelier, M. Guevara, L. Tarrason, and A. Clappier, "A novel approach to screen and compare emission inventories," *Air Qual., Atmos. Health*, vol. 9, no. 4, pp. 325–333, May 2016.

[9] Z. Yan, B. Gainey, J. Gohn, D. Hariharan, J. Saputo, C. Schmidt, F. Caliari, S. Sampath, and B. Lawler, "A comprehensive experimental investigation of low-temperature combustion with thick thermal barrier coatings," *Energy*, vol. 222, May 2021, Art. no. 119954.

[10] C. Huang, A. F. Molisch, R. He, R. Wang, P. Tang, and Z. Zhong, "Machine-learning-based data processing techniques for vehicle-to-vehicle channel modeling," *IEEE Commun. Mag.*, vol. 57, no. 11, pp. 109–115, Nov. 2019.

[11] J. Li, Q. Zhou, X. He, W. Chen, and H. Xu, "Data-driven enabling technologies in soft sensors of modern internal combustion engines: Perspectives," *Energy*, vol. 272, Jun. 2023, Art. no. 127067, doi: 10.1016/j.energy.2023.127067.

[12] J. Liu, C. Ulishney, and C. E. Dumitrescu, "Comparative performance of machine learning algorithms in predicting nitrogen oxides emissions of a heavy-duty natural gas spark ignition engine," in *Proc. Int. Conf. Appl. Energy*, vol. 29, 2021, p. 71.

[13] A. Yousefzadeh and O. Jahanian, "Using detailed chemical kinetics 3D-CFD model to investigate combustion phase of a CNG-HCCI engine according to control strategy requirements," *Energy Convers. Manage.*, vol. 133, pp. 524–534, Feb. 2017.

[14] H. Huang, D. Lv, J. Zhu, Z. Zhu, Y. Chen, Y. Pan, and M. Pan, "Development of a new reduced diesel/natural gas mechanism for dual-fuel engine combustion and emission prediction," *Fuel*, vol. 236, pp. 30–42, Jan. 2019.

[15] B. Gainey, Z. Yan, and B. Lawler, "Autoignition characterization of methanol, ethanol, propanol, and butanol over a wide range of operating conditions in LTC/HCCI," *Fuel*, vol. 287, Mar. 2021, Art. no. 119495.

[16] J. Gao, Y. Wu, and T. Shen, "On-line statistical combustion phase optimization and control of Si gasoline engines," *Appl. Thermal Eng.*, vol. 112, pp. 1396–1407, Feb. 2017.

[17] J. A. Caton, "Combustion phasing for maximum efficiency for conventional and high efficiency engines," *Energy Convers. Manage.*, vol. 77, pp. 564–576, Jan. 2014.

[18] J. Liu, Q. Huang, C. Ulishney, and C. E. Dumitrescu, "Comparison of random forest and neural network in modeling the performance and emissions of a natural gas spark ignition engine," *J. Energy Resour. Technol.*, vol. 144, no. 3, Mar. 2022, Art. no. 032310.

[19] J. Dornoff, F. Rodriguez. (2019). *Gasoline Versus Diesel: Comparing CO_2 Emission Levels of a Modern Medium Size Car Model Under Laboratory and On-Road Testing Conditions*. Accessed: Nov. 2023. [Online]. Available: https://theicct.org/publication/gasoline-versus-diesel-comparing-co2-emission-levels-of-a-modern-medium-size-car-model-under-laboratory-and-on-road-testing-conditions/

[20] F. J. J. S. Bai, "A machine learning approach for carbon di oxide and other emissions characteristics prediction in a low carbon biofuel-hydrogen dual fuel engine," *Fuel*, vol. 341, Jun. 2023, Art. no. 127578.

[21] F. J. J. S. Bai, K. Shanmugaiah, A. Sonthalia, Y. Devarajan, and E. G. Varuvel, "Application of machine learning algorithms for predicting the engine characteristics of a wheat germ oil–hydrogen fuelled dual fuel engine," *Int. J. Hydrogen Energy*, vol. 48, no. 60, pp. 23308–23322, Jul. 2023.

[22] Z. He, G. Ye, H. Jiang, and Y. Fu, "Vehicle emission detection in data-driven methods," *Math. Problems Eng.*, vol. 2020, pp. 1–13, Oct. 2020, doi: 10.1155/2020/4875310.

[23] C. Saleh, N. R. Dzakiyullah, and J. B. Nugroho, "Carbon dioxide emission prediction using support vector machine," *IOP Conf. Ser., Mater. Sci. Eng.*, vol. 114, Feb. 2016, Art. no. 012148, doi: 10.1088/1757-899x/114/1/012148.

[24] Y. Zhang, Q. Wang, X. Chen, Y. Yan, R. Yang, Z. Liu, and J. Fu, "The prediction of spark-ignition engine performance and emissions based on the SVR algorithm," *Processes*, vol. 10, no. 2, p. 312, Feb. 2022.
[25] K. Karunamurthy, A. A. Janvekar, P. L. Palaniappan, V. Adhitya, T. T. K. Lokeswar, and J. Harish, "Prediction of IC engine performance and emission parameters using machine learning: A review," *J. Thermal Anal. Calorimetry*, vol. 148, no. 9, pp. 3155–3177, May 2023.
[26] R. Yang, T. Xie, and Z. Liu, "The application of machine learning methods to predict the power output of internal combustion engines," *Energies*, vol. 15, no. 9, p. 3242, Apr. 2022, doi: 10.3390/en15093242.
[27] M.-T. Tran-Nguyen, L.-D. Bui, and T.-N. Do, "Decision trees using local support vector regression models for large datasets," *J. Inf. Telecommun.*, vol. 4, no. 1, pp. 17–35, Jan. 2020, doi: 10.1080/24751839.2019.1686682.
[28] B. Schölkopf, A. J. Smola, R. C. Williamson, and P. L. Bartlett, "New support vector algorithms," *Neural Comput.*, vol. 12, no. 5, pp. 1207–1245, May 2000.
[29] A. Arshad, S. Riaz, and L. Jiao, "Semi-supervised deep fuzzy C-mean clustering for imbalanced multi-class classification," *IEEE Access*, vol. 7, pp. 28100–28112, 2019, doi: 10.1109/ACCESS.2019.2901860.
[30] N. Niroomand, C. Bach, and M. Elser, "Robust vehicle classification based on deep features learning," *IEEE Access*, vol. 9, pp. 95675–95685, 2021, doi: 10.1109/ACCESS.2021.3094366.
[31] F. Grelier, *CO_2 Emissions Form Cars: The Facts; Technical Report; European Federation for Transport and Environment*. Brussels, Belgium: AISBL, 2018.
[32] N. Niroomand, C. Bach, and M. Elser, "Vehicle dimensions based passenger car classification using fuzzy and non-fuzzy clustering methods," *Transp. Res. Rec., J. Transp. Res. Board*, vol. 2675, no. 10, pp. 184–194, Oct. 2021, doi: 10.1177/03611981211010795.
[33] N. Niroomand, C. Bach, and M. Elser, "Segment-based CO_2 emission evaluations from passenger cars based on deep learning techniques," *IEEE Access*, vol. 9, pp. 166314–166327, 2021, doi: 10.1109/ACCESS.2021.3135604.
[34] N. Niroomand and C. Bach, "Estimating average vehicle mileage for various vehicle classes using polynomial models in deep classifiers," *IEEE Access*, vol. 12, pp. 17404–17418, 2024, doi: 10.1109/ACCESS.2024.3359990.
[35] *World Energy Outlook 2018*, Int. Energy Agency, Paris, France, 2018.
[36] *Federal Office for the Environment (FOEN)*. Accessed: Oct. 2023. [Online]. Available: https://www.bafu.admin.ch/bafu/en/home/topics/climate/state/data/greenhouse-gasinventory/
[37] *Swiss Federal Office of Energy (SFOE), CO_2 Emission Regulations for New Cars and Light Commercial Vehicles*. Accessed: Jan. 2024. [Online]. Available: https://www.bfe.admin.ch/bfe/en/home/efficiency/mobility/co2-emission-regulations-for-new-cars-and-light-commercial-vehicles.html
[38] *Swiss Federal Office of Energy (SFOE), Mobility Behavior of the Population*. Accessed: Feb. 2024. [Online]. Available: https://www.bfs.admin.ch/bfs/de/home/statistiken/mobilitaetverkehr/personenverkehr/
[39] A. Dimaratos, D. Tsokolis, G. Fontaras, S. Tsiakmakis, B. Ciuffo, and Z. Samaras, "Comparative evaluation of the effect of various technologies on light-duty vehicle CO_2 emissions over NEDC and WLTP," *Transp. Res. Proc.*, vol. 14, pp. 3169–3178, Jan. 2016.
[40] (2023). *Das Motorfahrzeuginformationssystem Der Eidgenossischen Fahrzeugkontrolle, MOFIS*. Accessed: Mar. 2019. [Online]. Available: https://www.experience-online.ch/de/9-case-study/2023-mofis
[41] *Bundesamt Für Strassen, ASTRA*. Accessed: Mar. 2019. [Online]. Available: https://www.astra.amin.ch/astra/de/home.html
[42] *Schweizer Partner Für Fahrzeugdaten*. Accessed: Mar. 2020. [Online]. Available: https://www.auto-i-dat.ch
[43] G. Forestier and C. Wemmert, "Semi-supervised learning using multiple clusterings with limited labeled data," *Inf. Sci.*, vols. 361–362, pp. 48–65, Sep. 2016.
[44] Y. Ren, X. Hu, K. Shi, G. Yu, D. Yao, and Z. Xu, "Semi-supervised denpeak clustering with pairwise constraints," in *Proc. 15th Pacific Rim Int. Conf. Artif. Intell.*, 2018, pp. 837–850.
[45] Y. Qin, S. Ding, L. Wang, and Y. Wang, "Research progress on semi-supervised clustering," *Cognit. Comput.*, vol. 11, no. 5, pp. 599–612, Oct. 2019.
[46] W. Shi, Y. Gong, C. Chris, Z. Ma, X. Tao, and N. Zheng, "Transductive semi-supervised deep learning using min-max features," in *Proc. Eur. Conf. Comput. Vis. (ECCV)*, Sep. 2018, pp. 299–315.
[47] G. Chen, "Deep transductive semi-supervised maximum margin clustering," 2015, *arXiv:1501.06237*.
[48] S. Riaz, A. Arshad, and L. Jiao, "A semi-supervised CNN with fuzzy rough C-mean for image classification," *IEEE Access*, vol. 7, pp. 49641–49652, 2019, doi: 10.1109/ACCESS.2019.2910406.
[49] L. Wang, M. Han, X. Li, N. Zhang, and H. Cheng, "Review of classification methods on unbalanced data sets," *IEEE Access*, vol. 9, pp. 64606–64628, 2021, doi: 10.1109/ACCESS.2021.3074243.
[50] T. M. Khoshgoftaar, C. Seiffert, J. V. Hulse, A. Napolitano, and A. Folleco, "Learning with limited minority class data," in *Proc. 6th Int. Conf. Mach. Learn. Appl. (ICMLA)*, Dec. 2007, pp. 348–353.
[51] *Schweizer Partner Fur Fahrzeugdaten*. Accessed: Jan. 2024. [Online]. Available: https://www.auto-i-dat.ch
[52] J. Montoya-Torres, O. Akizu-Gardoki, and M. Iturrondobeitia, "Measuring life-cycle carbon emissions of private transportation in urban and rural settings," *Sustain. Cities Soc.*, vol. 96, Sep. 2023, Art. no. 104658, doi: 10.1016/j.scs.2023.104658.

NAGHMEH NIROOMAND received the M.A. and Ph.D. degrees from Eastern Mediterranean University, Cyprus. She completed the I.A.P.M. Program at Queen's University, Canada, and the Ph.D. Program at SSPH+, Switzerland. She is currently a Techno-Energy Economist with the ZHAW Zurich University of Applied Sciences. She has been a Visiting Fellow with the Transport and Mobility Laboratory, EPFL Lausanne, and a Senior Scientist with Cambridge Resources International, USA. Prior to joining ZHAW, she was with the Automotive Powertrain Technologies Laboratory, Swiss Federal Laboratories for Materials Science and Technology (Empa). Her current research interests include vehicle fleet and operational analysis, retro-perspective analysis of vehicle-specific changes in the function of spatial technology and economic frame conditions, and exploring the impact of integrating electric cars and synthetic fuel into the existing infrastructure, as well as examining the connection between low and medium voltage grids.

CHRISTIAN BACH received the B.Sc. degree in automotive engineering from Bern University of Applied Sciences. He performed two internships at the Haagen-Smit Laboratory, California Air Resources Board, El Monte, CA, USA, to study zero and ultra-low emission technologies in the transport sector. He is currently the Head of the Chemical Energy Carriers and Vehicle Systems Laboratory, Swiss Federal Laboratories for Materials Science and Technology (Empa). He is also a Lecturer at ETH Zürich and a member of several expert groups in Switzerland.